2018 IEEE International Conference on Robotics and Automation (ICRA)
May 21-25, 2018, Brisbane, Australia

LASDRA: Large-Size Aerial Skeleton System with Distributed Rotor Actuation

Hyunsoo Yang, Sangyul Park, Jeongseob Lee, Joonmo Ahn, Dongwon Son and Dongjun Lee

Abstract— **Electrical motor and hydraulic actuation widely-used in robotics are "internal actuation" with their actuators sitting at the joint between two links. This internal actuation is fundamentally limiting to construct a large-size dexterously-articulated robot, since any external force (and its own link weight) is to be accumulated to the base multiplied by the moment arm length, requiring extremely strong/sturdy base actuator/structure as the system size increases. In this paper, we propose a novel robotic system, *LASDRA* (large-size aerial skeleton with distributed rotor actuation), which, by utilizing distributed rotors as "external actuation", can overcome this limitation of internal actuation and enables us to realize large-size dexterously-articulated robots. We present its design and modeling, joint locking strategy to increase its loading capability, and also a novel decentralized control scheme to allow for compliant operation with scalability against the number of links. Trajectory tracking and valve turning experiments are also performed to validate the theory.**

I. Introduction

Large-size robotic systems with dexterously-actuated limbs and skeleton structures have been the subject of our imagination, frequently witnessed in the form of mega-robots in numerous sci-fi movies and animations. Even so, physical realization of robotic systems with such large-size and dexterously-actuated many degree-of-freedom (DOF) motion has been very rare, and, even those realized far short from our imagination and the depictions. Some examples include: Kuka Titan 1000 [1] (6-DOF motion, electrical motor actuation, 3.6m height, 4.75ton weight), Kuratas [2] (30-DOF motion, hydraulic actuation, 4m height, 4.5ton weight), and Method 2 [3] (24-DOF motion, electrical motor actuation, 4.15m height, 1.6ton weight).

This mismatch, we believe, can be attributed to the fundamental limitation of the two most dominant actuation technologies in robotics: electrical motors and hydraulic actuation. More precisely, these two actuation technologies are all "internal actuation", that is, their actuators (e.g., rotational motor or hydraulic piston) are situated at the joint between two links. This then means that any external force acting on one of its links, including its own weight, is to be accumulated to the base, multiplied by the moment arm length from that (e.g., required control actuation quadratically increasing w.r.t. the link number - see Fig. 4 in Sec. II). This further implies that, to realize such a large-size robotic system, the base actuator should be extremely large and the base joint extremely sturdy to withstand even a small external load (or even only its own weight) through the long-reach of the large-size links. In fact, this fundamental limitation can be seen from the fairly heavy weight of all the aforementioned large-size robots (i.e., around 1ton weight for 2m height).

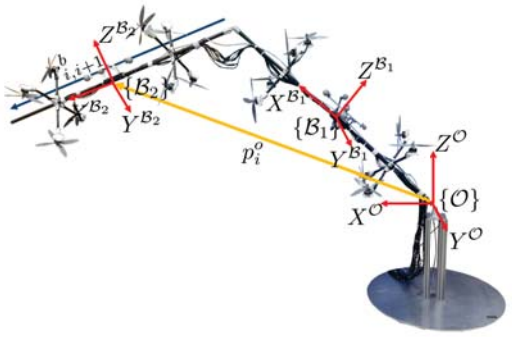

Fig. 1: Two-link LASDRA system consisting of two rigid links, each fully-actuated by distributed rotors, and spherical joints between the links to maximize motion dexterity.

In this paper, we propose a novel robotic system, **LASDRA** (large-size aerial skeleton with distributed rotor actuation), which, by utilizing the distributed reversible rotors as a means of "external actuation", can overcome those fundamental limitations of the electrical motor and hydraulic internal actuation technologies as stated above, and, consequently, enables us to realize a large-size and dexterously-articulated mechanical system. An example of this LASDRA system is depicted in Fig. 1, which consists of multiple rigid links, each fully-actuated in SE(3) by distributed rotors as designed in [4], and the spherical joints between the links to maximize its motion dexterity. Then, if some external force is on one of the links, it can be locally sustained by that very link (together with the weight of the link itself), as long as the actuation of the link is strong enough. In this way, we can avoid the issue of load accumulation to the base of the internal actuation. Of course, given the limitation of the currently-available rotor and power technologies, for some applications, it may be difficult to construct each link to be strong enough to withhold the required interaction wrenches. For this, we can utilize the strategy of joint locking, that is, by locking some spherical joints of the LASDRA system, external wrench on one link can be "spread" throughout the set of the locked links, thereby, increasing the loading capability of the LASDRA system while sacrificing some motion dexterity. This joint locking can be applied to render the LASDRA system as the combination of articulated segments, each composed of several joint-locked links. The target loading rating of the LASDRA system is also not as large as that of those large-size conventional robots mentioned above, although its size much larger than theirs (e.g., 10-20m size with 3-5kg loading rate).

The LASDRA system, due to its adoption of external distributed rotor actuation, is much lighter than its motor or hydraulic counterparts (e.g., less than 10kg for 3m height -

Research supported by the Basic Science Research Program (2015R1A2A1A15055616) of the National Research Foundation (NRF) funded by the Ministry of Science, ICT & Future Planning (MSIP), Korea.

The authors are with Department of Mechanical & Aerospace Engineering and IAMD, Seoul National University, Seoul, Republic of Korea.{yangssoo,sangyul,overjs94,ahnjmo1993,son3933,djlee}@snu.ac.kr

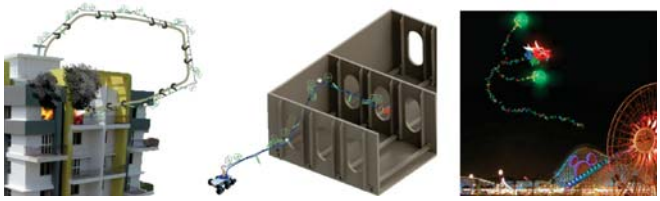

Fig. 2: Some envisioned applications of the LASDRA system: (a) fire-fighting in urban high-rise building (from the top); (b) painting task through narrow long horizontal space with partitions; and (c) large-size flying animating character in night sky with LED lights.

see Sec. V). It can also operate in a gravity-defying manner, allowing for applications, that require long-reach operation in narrow long space (e.g., painting of partitioned ship interior). The design of the LASDRA system, that consists of multiple links and spherical joints, is also amicable to modularization and easy to fold down, which, together with the light weight, would make the LASDRA system portable, suitable for deployment in densely-populated urban areas. The LASDRA system may operate tethered to power supply if long time operation and/or high loading capability is desired; or untethered with battery if necessary to fly high. Inheriting the backdrivability of rotor-actuated aerial platforms (e.g., [4], [5]), this LASDRA system is also capable of compliant interaction with external environments (e.g., impedance control possible). See Fig. 2 for some envisioned applications of the LASDRA system.

This LASDRA system stems from the line of our previous research on the aerial manipulation: quadrotor-tool and quadrotor-arm systems [6], [7], SmQ (spherically-connected multiple quadrotors) system [5], and, particularly, ODAR (omni-directional aerial robot) system [4], [5]. The idea of using multiple quadrotors as actuators was also explored in [8]–[10], yet, all these works [8]–[10] consider only the case of arranging the quadrotors (and their rotors) all co-linear, aiming to increase the vertical payload, not to achieve dexterous articulation. Recently, large-size pneumatic soft robots were proposed in [11], [12], yet, due to their relying on pneumatic actuation and soft structure, their loading capability is limited with the precise control difficult as well. Also, related are the works of [13] (flying humanoid with thrusters) and [14] (rigid object manipulated together with robot arm and freely-rotating quadrotor), yet, in both of them, the thrusters or quadrotors are utilized only for flying modality or to assist the robot manipulating the rigid object, not to attain dexterous articulation of structures as done in this paper. In fact, to our knowledge, the idea of utilizing the rotors used in aerial robotics as distributed actuators to achieve a large-size dexterously-articulated structure while recognizing its nature of external actuation to overcome the fundamental limitation of the conventional internal actuation to realize such large-size dexterous structures is proposed in this paper for the first time.

The rest of the paper is organized as follows. In Sec. II, some properties of external actuation are discussed as compared to internal actuation. The LASDRA system is then introduced in Sec. III with its kinematic and dynamic modeling. The decentralized control of the LASDRA system exploiting the backdrivability of rotor actuation is derived in Sec. IV. Experimental results of the motion and interaction control the LASDRA system are presented in Sec. V. Sec. VI concludes the paper with concluding remarks.

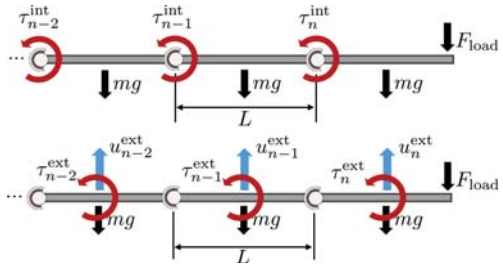

Fig. 3: Illustration of the n-link system with internal actuation (top: with joint torque τ^{int}_k) and external actuation (bottom: with force and torque, $(u^{\text{ext}}_k, \tau^{\text{ext}}_k)$, generated by distributed rotors).

II. Internal Actuation vs External Actuation

The LASDRA system utilizes distributed rotors as means of external actuation. These rotors render each of the links fully-actuated in SE(3), thereby, alleviating the issue of load accumulation toward the base, a fundamental limitation of internal actuation for constructing large-size dexterously-articulated structures. To better see this, consider the n-link articulated system as shown in Fig. 3, which fully stretches horizontally with the same mass m and length L and experiences a downward load F_{load} at the tip of its distal link. Then, with the internal actuation (e.g., electrical motors), the required control torque τ^{int}_k to sustain the load can be computed to be:

$$\tau^{\text{int}}_k = \sum_{j=k}^{n}(j-k+\frac{1}{2})mgL + (n-k+1)F_{\text{load}}L \quad (1)$$

whereas, with the external actuation (bottom of Fig. 3), to sustain the load F_{load}, the control torque and force $(\tau^{\text{ext}}_k, u^{ext}_k)$ should satisfy the following relation:

$$\tau^{\text{ext}}_k = (n-k+\frac{1}{2})mgL + F_{\text{load}}L - \left(\sum_{j=k}^{n} u^{\text{ext}}_j - \frac{1}{2}u^{\text{ext}}_k\right)L \quad (2)$$

Now, assume first that we do not use control force (i.e., $u^{ext}_k = 0$). Even in this case, we can see from (1)-(2) that, for the case of internal actuation, the required control torque is quadratically increasing w.r.t. the link number n, whereas, for the case of external actuation, it only increases linearly w.r.t. n. Even more striking contrast appears if we consider the case of external actuation with local gravity compensation (i.e., $u^{ext}_k = mg$), for which we have $\tau^{\text{ext}}_k = F_{\text{load}}L$ (i.e., constant!), $\forall k = 1, ..., n$. See Fig. 4 for this analysis for a ten-link system. This then unequivocally shows that the conventional internal actuation is fundamentally limiting to construct large-size articulated systems, and the external actuation would be more proper for that purpose by providing completely different mechanism to propagate the load throughout the system as compared to that of the internal actuation.

The above analysis also shows that, with the external actuation, each link would need to be strong enough to withstand the contact load, individually. Given the currently-available rotor and power technologies, this may not be easy to attain for some applications. For this, we can utilize the joint locking strategy, that is, by locking some of the spherical joints, some large external load can be spread through the set of the locked links, thereby, increasing the loading capability of the LASDRA system while sacrificing some

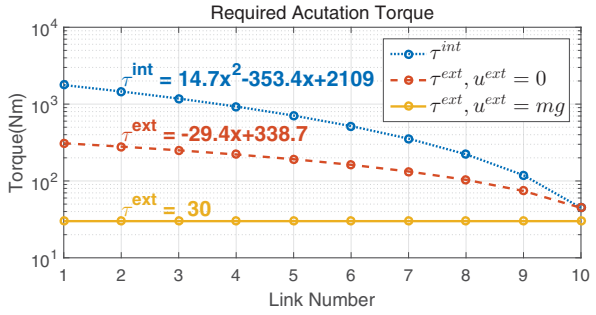

Fig. 4: Required control torque to sustain the load in Fig. 3 with $F_{load} = 20N$, $m = 1kg$, $L = 1.5m$: 1) with internal actuation (blue: quadratic w.r.t. link number); 2) with external actuation with no control force $u_i^{\text{ext}} = 0$ (red: linear w.r.t. link number); and 3) with external actuation with $u_i^{\text{ext}} = mg$ (yellow: constant regardless link number).

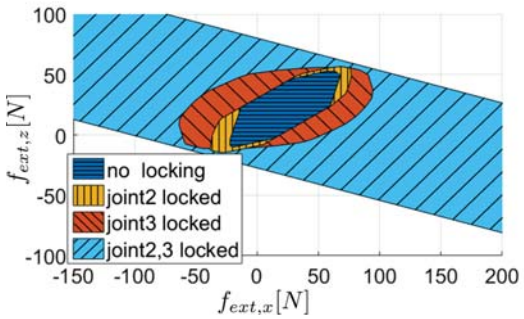

Fig. 5: Space of the sustainable interaction force at the tip of the third link of the planar LASDRA system with or without joint locking: only locking of the second and third joints are considered.

motion dexterity. See also Fig. 6 for a joint design example for this. To show the efficacy of the joint locking strategy, we perform a simulation, where a three-link LASDRA system is situated in its sagittal plane (i.e., (x, z)-plane) with the pitch angle of the three links given by ($\theta_1 = 60°$, $\theta_2 = 15°$, $\theta_3 = -30°$). We also set the link mass $m = 2kg$, link length $L = 1.5m$, and maximum rotor thrust $9.7N$, all similar to the experimental setup in Sec. V. We can then compute the interaction force at the third-link tip, that can be sustained with or without joint locking. We only consider the locking of the second and/or third joints for this. The space of this sustainable interaction force is then shown in Fig. 5, from which we can see that, with the joint locking, the space becomes much larger, manifesting the efficacy of the joint locking. Note also from Fig. 5 that, with the joint locking, even with bounded rotor actuation, the system can still endure infinite force along some direction, which turns out to be the singularity direction along with no motion possible.

III. System Description and Modeling

The LASDRA system consists of multiple rigid links, each fully-actuated in SE(3) with distributed rotors as the means of external actuation, and spherical joint between the links to maximize its motion dexterity. See Fig. 1 for an example of the two-link LASDRA system. To render each link to be fully-actuated, in this paper, we adopt the optimal design of ODAR [4], [15], which utilizes asymmetrically-attached eight rotors to attain the control actuation enough to fly only with onboard battery and also to provide control redundancy to circumvent the issue of sluggish direction change of the reversible ESC (electronic speed control) with sensor-less BLDC (brush-less direct current) motors (i.e., actuation singularity due to zero-crossing [15]). Of course, the results presented in this paper are by no means bound to a specific link design, and a general design optimization framework of the LASDRA system given a set of target tasks is a topic for future research.

The control wrench $(u_i^b, \tau_i^b) \in \text{se}(3)$ of the i-th link of the LASDRA system expressed in the body-frame $\mathcal{B}_i$ of the i-th link is then given by

$$\begin{bmatrix} u_i^b \\ \tau_i^b \end{bmatrix} = B_i \lambda_i$$

where $B_i \in \Re^{6\times 8}$ is the (constant) thrust mapping matrix determined by the geometric distribution of the rotors and $\lambda_i \in \Re^8$ is the thrust vector generated by the eight rotors. In Sec. IV, we will design the control (u_i^b, τ_i^b) for each link given the system-level control objective. This (u_i^b, τ_i^b) is then assigned to the eight-rotor thrust $\lambda_i \in \Re^8$ s.t.,

$$\lambda_i = B_i^\dagger u_i^b + N_{B_i} u_{N,i}^b$$

where $B_i^\dagger \in \Re^{8\times 6}$ is the pseudo-inverse of B_i, $N_{B_i} \in \Re^{8\times 2}$ is the null space matrix of B_i and $u_{N,i}^b \in \Re^2$ is the components of λ_i in N_{B_i}. We choose $u_{N,i}^b$ to be the infinite-norm minimizer (to avoid rotor saturation) under the selective mapping (to avoid rotor zero-crossing), for which we utilize the closed-form expressions provided in [15] as well. This issue of thrust mapping is not the main concern of this paper and we refer readers to [15] for more details on that.

All the links of the LASDRA system are connected via the spherical joint between them to avoid any restriction on the rotational motion, thereby, maximizing the system motion dexterity. Commercially-available spherical joints, yet, have fairly limited rotation range [5]. Due to this limitation, here, we instead adopt PVC (polyvinyl chloride) ropes to connect the two links - see Fig. 6. With the ropes tightened, these PVC ropes turn out to behave similar enough to the spherical joint (i.e., high-stiffness position constraint with low-compliance rotation motion) - see the experimental results in Sec. V. We also design the joint locking mechanism as shown in Fig. 6: with the branched ball-and-socket mechanism, it can lock the two links at a certain relative angle with each other. In this paper, we do not implement this joint locking, although analyzed in Sec. II. Mechanism design for this joint locking and its experimental validation is the topic of our ongoing research.

With the spherical joint (via the PVC ropes), we then have the following kinematic constraint and its time derivative for each link:

$$p_i^o = \sum_{j=1}^{i-1} R_j r_{j,j+1}^b + R_i r_{i,ci}^b, \quad i = 1, ..., n \tag{3}$$

$$\dot{p}_i^o = -\sum_{j=1}^{i-1} R_j S(r_{j,j+1}^b) w_j^b - R_i S(r_{i,ci}^b) w_i^b =: J_i w^b \tag{4}$$

where $p_i^o, \dot{p}_i^o$ is the center-of-mass position and velocity of the i-th link expressed in the inertial frame $\mathcal{O}$, $w_i^b \in \Re^3$ is its angular velocity expressed in $\mathcal{B}_i$, $w^b := [w_1^b; \cdots; w_n^b] \in \Re^{3n}$ is the combined angular velocity of all the links, $R_i \in$ SO(3) is the rotation matrix from $\mathcal{B}_i$ to $\mathcal{O}$, $r_{i,i+1}^b \in \Re^3$ is the position vector from the i-th joint to the $(i+1)$-th joint

Fig. 6: Joint designs of the LASDRA system: spherical joint with PVC ropes connecting two links to maximize motion dexterity (left); branched ball-and-socket mechanism for joint locking (right).

expressed in the body frame $\mathcal{B}_i$ with c_i denoting the center-of-mass position of the i-th link, and $n \geq 1$ is the number of the links, $J_i \in \Re^{3\times 3n}$ is Jacobian for translation velocity, $S(\cdot) \in \Re^{3\times 3}$ is the skew-symmetric matrix mapping of the vector such as $S(a)b = a \times b$. Throughout the paper, x^o and x^b of the i-th link represent x expressed in $\mathcal{O}$ and $\mathcal{B}_i$. Due to this constraint (3), the motion of each link reduces from SE(3) to SO(3) (relative to its preceding link), and the motion-DOF of the n-link LASDRA system from $6n$ to $3n$.

The LASDRA system is envisioned to be constructed with many links and with various topological structures. Due to this reason, for the modeling, control and analysis of the LASDRA system, we aim to rely on the Newton-Euler formulation (i.e., maximal coordinates [16]) rather than the Lagrange formulation (i.e., generalized coordinates [16]) to make the results scalable and also possibly decentralized (see Sec. IV). This Newton-Euler dynamics formulation is then given by: for each link of the LASDRA system,

$$m_i\ddot{p}_i^o + m_i g e_3 = R_i u_i^b + R_i f_i^b - R_{i+1} f_{i+1}^b \tag{5}$$

$$\mathcal{I}_i\dot{w}_i^b + S(w_i^b)J_i w_i^b = \tau_i^b + S(r_{ci,i}^b)f_i^b - S(r_{ci,i+1}^b)R_{i+1}^i f_{i+1}^b \tag{6}$$

where $m_i \in \Re$ and $\mathcal{I}_i \in \Re^{3\times 3}$ are the mass and the moment of inertia of the i-th link, $u_i^b, \tau_i^b \in \Re^3$ are the control force and the torque expressed in $\mathcal{B}_i$, $f_i^b \in \Re^3$ is the internal force applied to the preceding link side of i-th link and $e_3 = [0; 0; 1]$ is the z-directional basis vector. Since the spherical joint allows free rotation, the internal wrench in (5)-(6) is only the internal force f_i, f_{i+1}. In this paper, we also assume the interaction with external environment takes place only at the last n-th link possibly with some end-effector attached there. Then, the dynamics of the n-th link will still be given by (5)-(6), yet, the internal force only from the $(n-1)$-th link and the external force f_{ext} acting on that.

IV. Decentralized Impedance Control Design

We envision the LASDRA system to be constructed with many links in various topology. For this, it is desirable to design the control to be scalable and modular, particularly for commercialization. This then suggests the direction of decentralized control. At the same time, the rotor-actuated aerial platforms are known to be backdrivable [5]. This then means that each link of the LASDRA system is not only fully-actuated but also backdrivable, thus, it would be rather straightforward to attain its impedance control for compliant interaction, which then would allow for not only the stable interaction with external environment but also the prevention of excessive internal force build-up at the spherical joints. Along this reasoning, here, we design the decentralized impedance control of the LASDRA system, and also analyze some of its important theoretical properties. For this, we also adopt high-stiffness impedance control for the rotational motion, as it completely specifies the configuration of the LASDRA system with the spherical joints, whereas high-compliance (i.e., low-stiffness) control for the translational motion to reduce the internal force at the spherical joints.

We then design the decentralized impedance control for each link as follows: given the desired orientation $R_{i,d} \in$SO(3) and its resultant position $p_{i,d} \in \Re^3$ from (3) (i.e., $p_{i,d}^o = \sum R_{i,d} r_{j,j+1}^b + R_{i,d} r_{i,ci}^b$), which are formulated from the high-level desired behavior of the LASDRA system,

$$u_i^b = R_i^T[m_i g e_3 + m_i\ddot{p}_{i,d}^o + k_d\dot{e}_{p,i} + k_p e_{p,i}] \tag{7}$$

$$\tau_i^b = w_i^b \times \mathcal{I}_i w_i^b - k_R e_{R,i} - k_w e_{w,i} - k_I e_{I,i} - \mathcal{I}_i(S(w_i)R_{i,d}^i w_{i,d}^b - R_{i,d}^i\dot{w}_{i,d}^b) \tag{8}$$

where $e_{p,i} := p_i^o - p_{i,d}^o \in \Re^3$ is the position error, $e_{R_i} := (R_{i,d}^T R_i - R_i^T R_{i,d})^\vee \in \Re^3$ the rotation error, $e_{w_i} := w_i^b - R_i^T R_{i,d} w_{i,d}^b \in \Re^3$ the angular velocity error, $e_{I,i} = \int e_{w,i} + \gamma e_{R,i} dt \in \Re^3$ the error integral, $k_p, k_d, k_R, k_w, k_I, \gamma \in \Re$ are control gains and $R_{i,d}^i := R_i^T R_{i,d}$. Note that the control (7)-(8) are decentralized, as it only includes the its own link state information $(p_i^o, R_i, \dot{p}_i^o, w_i^b)$ and feedforward terms available to all the links.

Then, the error dynamics can be derived by applying the control inputs (7)-(8) to the link dynamics (5)-(6) s.t.,

$$m_i\ddot{e}_{p,i} + k_d\dot{e}_{p,i} + k_p e_{p,i} = R_i f_i^b - R_{i+1} f_{i+1}^b \tag{9}$$

$$\mathcal{I}_i\dot{e}_{w,i} + k_w e_{w,i} + k_R e_{R,i} + k_I e_{I,i} = S(r_{ci,i}^b)f_i^b - S(r_{ci,i+1}^b)R_{i+1}^i f_{i+1}^b \tag{10}$$

As mentioned above, with the spherical joint constraint, $SE(3)$ dynamics can be reduced into $SO(3)$ rotation dynamics, thus, this error dynamics (9)-(10) can be reduced to e_{w_i}-dynamics. For this, we rewrite $e_{p,i}$ as a function of w_i, R_i using the spherical joint constraint (3) s.t.,

$$\dot{e}_{p,i} = R_i S(e_{w,i}) r_{i,ci}^b + R_i S(R_{i,d}^i w_{i,d}^b)(I - R_{i,d}^i) r_{i,ci}^b + \sum_{j=1}^{i} R_j S(e_{w,j}) r_{j,j+1}^b + R_j S(R_{j,d}^j w_{j,d})(I - R_{i,d}^i) r_{j,j+1}^b \tag{11}$$

The reduced rotational error dynamics can then be obtained by recursively substituting the internal force f_i in (10) by (9) and $e_{p,i}$ by (11) from the link n to 1. After substituting it, by collecting the n-links reduced rotational error dynamics, the total rotational dynamics can be expressed as following matrix and vector form:

$$M\dot{e}_w + (K_w + K_d + C(w^b))e_w + K_R e_R + K_I e_I = D - C(R^T R_d w_d^b)e_w \tag{12}$$

where $M, C(w^b) \in \Re^{3n\times 3n}$ are the combined inertia and Coriolis-like matrix, $K_d, K_w \in \Re^{3n\times 3n}$ are gain matrices and $D \in \Re^{3n\times 1}$ is the disturbance vector from metric difference between e_p, e_w and $w^b, w_d^b, e_w, e_R, e_I \in \Re^{3n}$ are the combined angular velocities and error vectors of n-links and $R = \text{diag}(R_1, \cdots, R_n), R_d = \text{diag}(R_{1,d}, \cdots, R_{n,d}) \in \Re^{3n\times 3n}$ are the block diagonal matrix of R_i and $R_{i,d}$ respectively. Expression of each matrices are summarized in appendix. Note that, in the matrices of (12), all the matrices are symmetric except C.

Proposition 1 *The error dynamics* (12) *possesses the following properties:*

1) $\dot{M} - 2C(w^b)$ *is a skew-symmetric and* $\dot{M} = C(w^b) + C^T(w^b)$.
2) K_d *is positive semi-definite.*
3) *If* $\Psi_i = \frac{1}{2}tr(R_{i,d}^T R_i - R_i^T R_{i,d}) < 1$*, then the disturbance vector* $D \in \Re^{3n\times 3n}$ *satisfies*
$$||D|| \leq c||e_R||$$
where $\gamma > 0$ *is a constant.*
4) *The derivative of rotation error satisfies the following inequality.*
$$||\dot{e}_R|| \leq ||e_w||$$
5) *The Coriolis matrix* $C \in \Re^{3n\times 3n}$ *satisfies*
$$||C(w^b)e_w|| \leq c_w||w^b|| \cdot ||e_w||,$$
$$||C(R^T R_d w_d^b)e_w|| \leq \eta_{w_d}^b||e_w||$$
where $c_w, \eta_{w_d} > 0$ *are the positive constants.*

Proof:
1) This can be easily shown by using the M and $C(w)$ in appendix.
2) As shown in appendix, the symmetric matrix $K_d = k_d J^T J$ where J is lower triangular matrix. Then, $x^T K_d x = (Jx)^T(Jx) \geq 0$ for all x.
3) We can write $R_{i,d}^i = \exp\hat{x} \in SO(3)$ where $\exp(\cdot)$ is the matrix exponential and $x \in \Re^3$ is the instantaneous rotation axis from Rodrigues formula [17]. Then, we have
$$(I - R_i^T R_{i,d}) = \sin||x||\frac{S(x)}{||x||} + (1 - \cos||x||)\frac{S(x)^2}{||x||^2}$$
Using the above relation, the inequality is given by
$$||(I - R_i^T R_{i,d})r_i|| \leq \sin||x||\zeta$$
where $\zeta > 0$ is a positive constant. Here, we utilize a inequality s.t., $\sin||x|| \geq 1 - \cos||x||$ for $||x|| < \pi/2$, which is equivalent to $\Psi_i < 1$. On the other hand, the error e_R can be written as $e_R = \sin||x||$. As a result, all the terms in D are bounded by $||e_R||$.
4) Please refer [18].
5) In the expression of $C_{i,j}$, $S(r_{i,i+1}^b)$ is a constant and $R_i \in SO(3)$ is bounded due to $\det(R) = 1$. And the desired angular velocity $w_{i,d}^b$ is also bounded. Therefore, $C(R^T R_d w_d^b)$ is bounded with its maximum eigenvalues are smaller than η_{w_d}. Next, since $C(w^b)e_w$ is a function of w^b and e_w, the inequality of $C(w^b)e_w$ can be easily shown with the proper constant c_w. ■

The stability of the proposed decentralized control without external force (i.e., $f_{ext} = 0$) is verified in the following theorem with the properties in the Prop. 1. We then analyze the stability with the external force later.

Theorem 1 *Consider the* n*-link LASDRA system with its dynamics of each links are given by* (5)-(6) *and the external force* $f_{ext} = 0$*. Then,* $(e_R, e_w, e_p) \to (0, 0, 0)$ *asymptotically and the internal force* f_i^b *converges to* 0 *with the decentralized control input* (7)-(8)*.*

Proof: Define Lyapunov candidate function
$$V = \frac{1}{2}e_w^T M e_w + K_R\Psi(R_d, R) + \gamma e_R^T M e_w + K_I\frac{1}{2}e_I^T e_I$$
where $\Psi = \sum_{i=1}^n \frac{1}{2}\text{tr}(R_{i,d}^T R_i - R_i^T R_{i,d})$ is the summation of Ψ_i and γ is a constant. Then, from $e_{I,i} = \int e_{w,i} + \gamma e_{R,i}dt \in \Re^3$, (12) and skew-symmetry of $\dot{M} - 2C(w)$, the time derivative of V is derived s.t.
$$\begin{aligned}\dot{V} = e_w^T\left\{-(K_w + K_d + C(R^T R_d w_d))e_w + D\right\}\\ - \gamma e_R^T(-\dot{M} + C(w) + K_w + K_d + C(R^T R_d w_d))e_w\\ + \gamma\dot{e}_R^T M e_w - \gamma e_R^T(K_R e_R - D)\end{aligned}$$
From the Prop. 1, $\dot{V}$ satisfy following inequality
$$\begin{aligned}\dot{V} \leq -(k_w - \eta_{w_d} - \gamma\lambda_{M,M})||e_w||^2 - \gamma(k_R - c)||e_R||^2\\ - (k_w - c - \eta_{w_d} - c_w||w^b||)||e_w|| \cdot ||e_R||\end{aligned}$$
where $\lambda_{M,M}$ is the maximum eigenvalue of M. In the above inequality, at $t = 0$, if k_w is large enough, then the time derivative of V satisfies $\dot{V}(0) \leq 0$ which is equivalent with $||e_w(t)|| \leq ||e_w(0)||$. Therefore, the angular velocity satisfy following triangle inequality
$$||w^b(t)|| - ||R^T R_d w_d^b(t)|| \leq ||w^b(0)|| + ||R^T R_d w_d^b(0)||$$
Due to the boundedness of $w_d^b(t)$, the angular velocity is also bounded. As a result, $\dot{V}$ is the negative semi-definite function which implies $(e_w, e_R) \to (0, 0)$. This Lyapunov stability only represents the stability of the rotational dynamics. Therefore, we also need to check the stability of the translational dynamics which is given by the translational error dynamics (9). For this, from $(e_w, e_R) \to (0, 0)$ and the definition of $e_{p,i}$, we have $(\dot{e}_{p,i}, e_{p,i}) \to (0, 0)$. Therefore, the internal force f_n converges to zero as left hand side of (9) converges to zero. Next, for the $(n-1)$-th link, the left hand side of the error dynamics converge to zero and the internal force f_n also converge to zero, thus $f_{n-1} \to 0$. This concludes that the internal force f_i converge to zero by inductive way. ■

We can see that the integral term $K_I e_I$ is cancelled out in the inequality of $\dot{V}$. Therefore, the decentralized control without the integral term, i.e., $k_I = 0$, the stability is also preserved. Here, we employ the integral term to compensate un-modelled error such as rotor thrust calibration error, rotor allocation error, etc. However, in the case of the interaction task, the integral control may induce the actuator saturation problem, thus we set the integral control gain to small enough or zero for the interaction task.

Since the conventional robotic arm is based on the internal actuation, the perfect tracking control is impossible with the proposed decentralized framework because the reaction force also exists between each link via the control action. To cancel out this reaction force, the state information of the adjacent links are required. On the other hand, the LASDRA system can independently actuate thanks to the external actuation nature. In addition, as compared to the case of internal actuation, for the LASDRA system, each link requires smaller control wrench and experience smaller deflection when there exists an external force as mentioned in Sec. III. This is also the case for the decentralized control framework and described in the following corollary.

Corollary 1 *Consider the external force* f_{ext} *is applied to the* n*-th link with the control input for the* 1 *to* $n-1$ *link are* (7)*,* (8)*.*

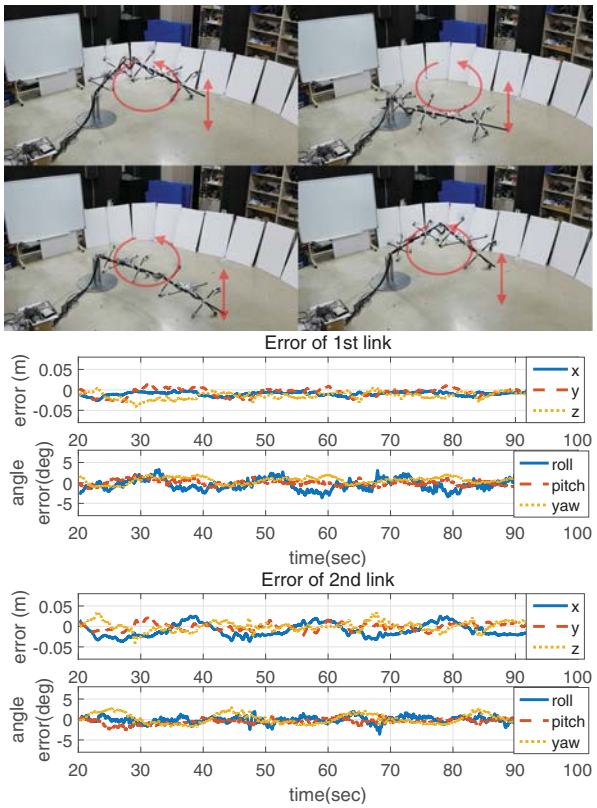

Fig. 7: Snapshots and position/rotation tracking errors of the trajectory tracking experiment.

1) *If the external force f_{ext} is known (e.g., force sensor), then $(e_R, e_w, e_p) \to (0,0,0)$ with following modified control input for last link*

$$R_n u_n^{b*} = R_n u_n^b + f_{ext} \tag{13}$$

$$\tau_n^{b*} = \tau_n^b - S(r_{cn,n+1}^b) f_{ext} \tag{14}$$

2) *If the external force f_{ext} is unknown, then the error (e_R, e_w, e_p) are bounded with control input* (7), (8)

Proof:

1) The error dynamics (9)-(10) are same with the control input (13)-(14). Therefore, according to Thm. 1, the errors (e_R, e_w, e_p) converge to zero.
2) The error dynamics with the external force is modified from (12)

$$M\dot{e}_w + (K_w + K_d + C(w^b))e_w + K_R e_R + K_I e_I = D - C(R^T R_d w_d^b)e_w + S_R f_{ext} \tag{15}$$

where the external force mapping matrix $S_R \in \Re^{3n\times 3}$ is defined as

$$S_R := [S(r_{1,2}^b)R_1^T; S(r_{2,3}^b)R_2^T; \cdots, S(r_{n,n+1}^b)R_n^T]$$

Then, the bounded additional term $(e_w^T + \gamma e_R^T)S_R f_{ext}$ is added into $\dot{V}$. According to the Th. 1, $\dot{V}$ is negative definite, thus, with the bounded external force f_{ext}, the errors (e_w, e_R, e_p) are ultimately bounded. ∎

Similar to the analysis in Sec. II, we assume the steady state case for Cor. 1, i.e., $e_w, w^b = 0$ and $\dot{f}_{ext} = 0$, then, due to the integral term, the error is given as $e_R = 0$ and

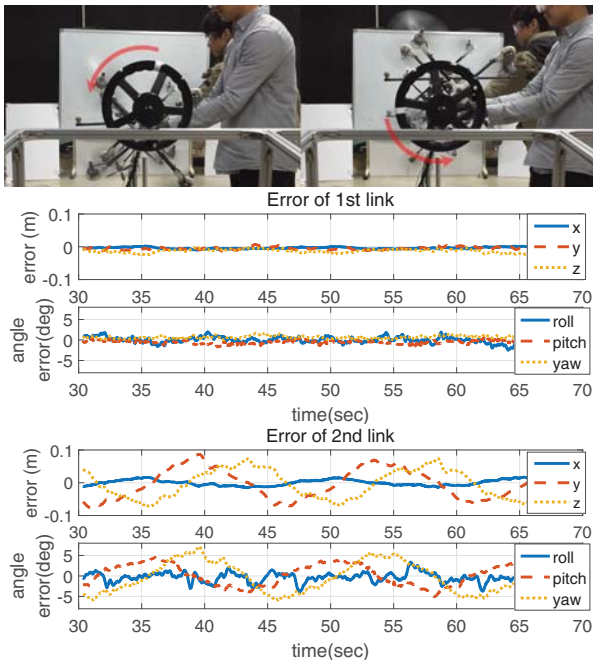

Fig. 8: Snapshot and position/rotation deviation from their nominal values due to the control compliance during the valve turning experiment.

the integral term is given as $e_I = K_I^{-1} S_R f_{ext}$ from (15). This result implies that the required control input u_i^b, τ_i^b only depend on the i-th link state R_i and geometry $r_{i,i+1}^b$ with the decentralized control framework while the internal actuation system accumulates the force as explained in Sec. II.

V. Experiments

We implement the two-link LASDRA system as shown in Fig. 1 with the PVC-rope spherical joint in Fig. 6. Each link is also constructed following the design of [4], [15]. The length of each link is 1.5m, making the height of the LASDRA system 3m. See Sec. III and [4], [15] for more details. Each link of the LASDRA system is then equipped with MCU (micro-controller unit), which communicates with the reversible ESCs, IMU attach on that link and also with the master computer. MOCAP is used to measure the position and orientation of each link, which is then fused with the IMU in the MCU on each link via the nonlinear complementary filtering [19]. Ground AC power unit is used to continuously supply power to the LASDRA system in a tethered manner although the operation using onboard battery is also possible [15]. Including all the components, cables, etc., the two-link LASDRA system weighs less than 10kg for the height of 3m, much lighter than other large-size robots mentioned in Sec. I.

Two experimental verifications are performed for this two-link LASDRA system with the decentralized control presented in Sec. IV: 1) trajectory tracking and 2) valve turning. First, for the tracking experiment, we choose the following desired trajectory for each link: with $(\phi_i, \theta_i, \varphi_i) \in \Re^3$ being the roll/pitch/yaw angles, $(\phi_1(t), \theta_1(t), \varphi_1(t)) = (0, -22.5 - 17.5\cos(\frac{\pi}{10}t), -19\sin(\frac{\pi}{10}t))$ and $(\phi_2(t), \theta_2(t), \varphi_2(t)) = (0, -5\cos(\frac{\pi}{10}t), 19\sin(\frac{\pi}{10}t))$. We then compute the desired position trajectory for (7)-(8) applying the spherical joint constraint (3). The results are shown in Fig. 7, where we can see that the LASDRA system can track the desired trajectory

fairly well, with the RMS (root-mean-square) position/angle errors of the first and second links being (2.25cm,1.85°) and (2.29 cm,1.59°), respectively.

The second valve turning experiment is to show the compliance of the proposed decentralized controller in Sec. IV. For this, no force sensor or force estimator are used. The period of the valve turning is 15sec. The results are shown in Fig. 7 and Fig. 8, where we can see that the LASDRA system can compliant and stably perform the valve turning task using the compliant behavior provided by our decentralized control (7)-(8), with RMS position/angle deviations of the first and second links from their nominal values being (1.59cm,1.28°) and (6.35cm, 5.70°), respectively. Here, note that the larger deviation of the second (distal) link as compared to that of the first (proximal) link. This is because the effect of the external force attenuates throughout the LASDRA system from the distal to proximal links as explained in Sec. II and Sec. IV. This larger deviation of the second link may be reduced by using some feedforward control with force sensing/estimation, which, yet, may not be desirable for some applications, where compliance is more important than stiff motion tracking. Joint locking strategy may also be used to increase the valve turning force, which is the topic of our ongoing research and will be reported in a future publication.

VI. Conclusion

In this paper, we propose a novel LASDRA (large-size aerial skeleton based distributed rotor actuation) system, which consists of multiple rigid links, each fully-actuated in SE(3) by distributed rotors as designed in [4], and the spherical joints between the links to maximize its motion dexterity. By utilizing the distributed rotors as external actuation, this LASDRA system can attain large-size and dexterous-articulation at the same time, a feat impossible with conventional internal motor/hydraulic actuation due to the issue of load/weight accumulation to the base of the system, requiring often excessively strong/sturdy actuator/structure. The loading capacity of this LASDRA system essentially depends on the actuation strength of each link, which can also be increased via the joint locking strategy. We also present a novel decentralized control for this LASDRA system to attain compliant operation and scalability. Preliminary experiments (trajectory tracking and valve turning) are also performed to show the feasibility of this LASDRA system. Some possible future research topics include: 1) joint locking mechanism implementation and experimental validation; 2) design optimization of each link depending for target tasks; and 3) multi-sensor fusion for MOCAP-less operation of the LASDRA system (e.g., [20]).

References

[1] Kuka. `https://www.kuka.com/en-de/products/robot-systems/industrial-robots/kr-1000-titan`. Accessed: 2017-09-11.

[2] Suidobashi heavy industry. `http://suidobashijuko.jp/`. Accessed: 2017-09-11.

[3] Hankook mirae technology. `http://hankookmirae.tech/main/method.html`. Accessed: 2017-09-11.

[4] S. Park, J. Her, J. Kim, and D. J. Lee. Design, modeling and control of omni-directional aerial robot. In *Proc. IEEE/RSJ Int'l Conference on Intelligent Robots and Systems*, pages 1570–1575, 2016.

[5] H. N. Nguyen, S. Park, and D. J. Lee. Aerial tool operation system using quadrotors as rotating thrust generators. In *Proc. IEEE/RSJ Int'l Conference on Intelligent Robots and Systems*, pages 1285–1291, 2015.

[6] N-H. Nguyen, C. Ha, and D. J. Lee. Mechanics, control and internal dynamics of quadrotor tool operation. *Automatica*, 61:289–301, 2015.

[7] H. Yang and D. J. Lee. Dynamics and control of quadrotor with robotic manipulator. In *Proc. IEEE Int'l Conference on Robotics and Automation*, pages 5544–5549, 2014.

[8] D. Mellinger, M. Shomin, N. Michael, and V. Kumar. Cooperative grasping and transport using multiple quadrotors. In *Proc. Intl. Symposium on Distributed Autonomous Robotic Systems*, 2010.

[9] R. Oung and R. D'Andrea. The distributed flight array. *Mechatronics*, 21:908–917, 2011.

[10] M. Zhao, K. Kawasaki, X. Chen, S. Noda, K. Okada, and M. Inaba. Whole-body aerial manipulation by transformable multirotor with two-dimensional multilinks. In *Proc. IEEE Int'l Conference on Robotics and Automation*, pages 5175–5182, 2017.

[11] M. Takeichi, K. Suzumori, G. Endo, and H. Nabae. Development of giacometti arm with balloon body. In *Proc. IEEE Int'l Conference on Robotics and Automation*, pages 951–957, 2017.

[12] E. W. Hawkes, L. H. Blumenschein, J. D. Greer, and A. M. Okamura. A soft robot that navigates its environment through growth. *Science Robotics*, 2(8), 2017.

[13] D. Pucci, S. Traversaro, and F. Nori. Momentum control of an underactuated flying humanoid robot. *IEEE Robotics & Automation Letters*, 2017 (Accepted).

[14] N. Staub, M. Mohammadi, D. Bicego, D. Prattichizzo, and A. Franchi. Towards robotic magmas: multiple aerial-ground manipulator systems. In *Proc. IEEE Int'l Conf. on Robotics & Automation*, pages 1307–1312, 2017.

[15] S. Park, J. Lee, J. Ahn, M. Kim, G-H. Yang J. Her, and D. J. Lee. Odar: Aerial manipulation platform enabling omni-directional wrench generation. *IEEE/ASME Transactions on Mechatronics*, 2017 (Submitted).

[16] M. Kim, Y. Lee, Y. Lee, and D. J. Lee. Haptic rendering and interactive simulation using passive midpoint integration. *International Journal of Robotics Research*,36(12), 2017.

[17] R. M. Murray, Z. Li, and S. S. Sastry. *A Mathmatical Introduction to Robotic Manipulation*. CRC Press, 1994.

[18] F. Goodarzi, D. Lee, and T. Lee. Geometric nonlinear pid control of a quadrotor uav on se(3). In *Proc. European Control Conference*, pages 3845–3850, 2013.

[19] R. Mahony, T. Hamel, and J.M. Pflimlin. Nonlinear complementary filters on the special orthogonal group. *IEEE Transactions on Automatic Control*, 53(5):1203–1218, 2008.

[20] Y. Lee, J. Yoon, H. Yang, C. Kim, and D. J. Lee. Camera-gps-imu sensor fusion for autonomous flying. In *Proc. Int'l Conference on Ubiquitous and Future Networks*, pages 85–99, 2016.

Appendix

Expression of each matrix in the error dynamics (12) defined by:

$$M = \mathcal{I} + J^T m J, \quad C(w) = J^T m \dot{J}, \qquad K_d = k_d J^T J$$

where $\mathcal{I} = \text{diag}(\mathcal{I}_1, \cdots, \mathcal{I}_n) \in \Re^{3n\times 3n}$, $m = \text{diag}(m_1 I_3, \cdots, m_n I_3) \in \Re^{3n\times 3n}$, $J := [J_1; \cdots; J_n] \in \Re^{3n\times 3n}$. $C(R^T R_d w)$ in (12) has the same structure with $C(w)$ and the only difference is that w_i^b are substituted by $R_i^T R_{i,d} w_i^b$. Next, D is written as

$$D = J^T d$$

where $d = [d_1; \cdots; d_n] \in \Re^{3n}$. Here, $d_i \in \Re^3$ defined as

$$d_i = d_{i,i} r_{j,cj}^b + \sum_{j=1}^{i} d_{i,j} r_{j,j+1}^b$$

where its component $d_{i,j}$ is defined s.t.

$$d_{i,j} = \Big\{ m_i (S(R_{j,d}^j \dot{w}_{j,d}^b) + S(R_{j,d}^j w_{j,d}^b)^2) + k_d S(R_{j,d}^j w_{j,d}^b) + k_p I \Big\} (I - R_{j,d}^j)$$

with the diagonal gain matrices

$$K_w = k_w I_{3n}, \quad K_R = k_R I_{3n}, \quad K_I = k_I I_{3n}$$